

# Rational design solutions for deep excavations using soil nail wall systems

Ahmad Alkhdour<sup>1\*</sup>, Amjad A. Yasin<sup>1</sup>, Oleksii Tiutkin<sup>2</sup>

<sup>1</sup>*Al-Balqa Applied University, Al-Salt, Jordan*

<sup>2</sup>*Ukrainian State University of Science and Technologies, Dnipro, Ukraine*

\*Corresponding author: e-mail [a.alkhdour@bau.edu.jo](mailto:a.alkhdour@bau.edu.jo)

## Abstract

**Purpose.** The study aims to optimize the design and reduce soil nail length in deep excavations with a soil nail system in fast-draining soils. Additionally, it investigates the parameters influencing slope stability in fast-draining soils.

**Methods.** Integrating field and lab data with soil nail properties and advanced modeling, this study investigates how fixed nail length, inclination and spacing affect the stability of a 20 m-deep excavation in fast-draining soil.

**Findings.** The study findings reveal that optimal parameters, such as nail spacing and inclination angle, have been identified for reinforcing deep excavation walls, ensuring stability with minimal nail length. Notably, the stability of excavation walls can be achieved without the need to increase the length of the soil nails. The recommended parameters are characteristic of an 8-meter-long soil nail system, a 30-degree inclination angle, and a spacing of 1.5×1.5 meters.

**Originality.** This study presents a novel perspective on the structural characteristics of soil nails by determining emphasizing nail spacing, inclination angle, and fixed nail length. It offers a comprehensive framework for designing soil nail walls in fast-draining soils during deep excavations, contributing to advancements in open-cut excavation practices.

**Practical implications.** The study offers practical implications for designers involved in deep slope earthworks, enabling the development of efficient and rational design solutions that ensure excavation stability and prevent displacement during excavation while reducing costs and project duration.

**Keywords:** *deep excavation, parameters for soil nail walls, PLAXIS 2D Connect Edition v22, finite-element analysis, HS-model*

## 1. Introduction

The stability of deep excavations and slope faces is critical for both mining operations and structures built within geological formations. Geotechnical engineers have extensively studied various methodologies, particularly in slope stability analysis, to remove complex geological obstacles. Thorough analysis and effective management of deep earthworks are vital to prevent emergencies and maintain the load-bearing capacity of nearby structure [1]-[5].

Excavations can cause disturbances within soil layers, posing challenges to excavation stability, which are similar to those faced by slope stability systems.

Many researchers have contributed to numerous studies aimed at addressing the stability issues associated with soil and rock layers during cutting, excavation, and mining operations [6]-[9]. These studies have significantly benefited the mining and construction industries by developing support systems that ensure stability in excavations and slope faces. Excavations pose a significant contemporary challenge, as the risks escalate with increasing depth [10]. Ensuring the stability of excavations, especially those with steep vertical slopes, is crucial. The unloading of soil can result in rapid movements and a decrease in safety margins,

especially as the excavation deepens, leaving limited time for preventive measures [11]-[13].

A support system had to be found to maintain the stability of deep excavations with steep slopes to meet the requirements of both mining operations and construction projects [14]. The design of deep excavations is becoming more complicated, the requirements for their design and construction are being supplemented and growing, tighter limits for allowable displacements, and new construction methods that go beyond traditional design methods [15]. Traditional sustainability-oriented design approaches are no longer enough.

Designs now require controlling displacements and limiting movements [16]. It is required to change the approach to designing systems for fixing deep excavation, including the definition of permissible limits of movement, developing an optimal solution to maintain movements within acceptable values, and determining steps to mitigate the consequences in case of exceeding the allowable movements [17]. Excavation failures can result in displacements caused by various mechanisms that require appropriate safety factors to be implemented. Besides these factors, pre-failure movements can arise from multiple causes, which can be evaluated through the utilization of Finite Element Analysis (FEA) software programs [18]-[22].

Received: 31 May 2023. Accepted: 5 September 2023. Available online: 30 September 2023

© 2023. A. Alkhdour, A.A. Yasin, O. Tiutkin

Mining of Mineral Deposits. ISSN 2415-3443 (Online) | ISSN 2415-3435 (Print)

This is an Open Access article distributed under the terms of the Creative Commons Attribution License (<http://creativecommons.org/licenses/by/4.0/>), which permits unrestricted reuse, distribution, and reproduction in any medium, provided the original work is properly cited.

Despite the considerable research conducted on deep excavation stability and soil nailing techniques, the process of selecting an appropriate soil nail design system to improve the stability of fast-drying deep excavations remains a complex undertaking [23].

This study presents various design approaches to select an appropriate soil nail design system that enhances the stability of fast-drying deep excavations. The selection process involves utilizing soil nailing techniques and the PLAXIS 2D Connect Edition v22 software. The analysis encompasses crucial factors such as soil properties, excavation geometry, and other pertinent parameters that influence excavation stability.

The primary objective is to identify the most suitable soil nail design system capable of mitigating excessive movements during deep excavation by effectively addressing failure motions induced by stress within the support system. The study particularly focuses on key contributing factors to failures in this domain, including the influence of soil layer stiffness, strength, and variations in the geometric properties of the slope stabilization structure for deep excavations.

## 2. Case study, numerical model

### 2.1. Initial data of the project

The excavation site is situated in the city of Amman and is adjacent to a multi-story building on its southern side. The deep excavation faces share similar depths and geotechnical conditions. The length of the excavation on the western and southern sides measures 50.4 and 47.9 meters, respectively. The study focuses on a specific side presented in the excavation plan shown in Figure 1.

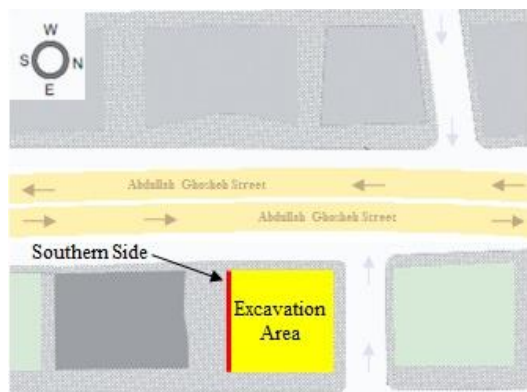


Figure 1. Excavation plan

In Figure 1, the excavation site is bordered by 10 m-wide roads to the north and east, a 20 m-wide main street to the west, and a multi-story building to the south, situated 10 m from the excavation area. The southern side was chosen for study based on investigations revealing comparable geotechnical conditions. The emphasis on the red-lined southern aspect holds significance due to its proximity to a vital multi-story building.

### 2.2. Excavation geotechnical condition

The soil at the site is layered at various depths, as determined from borehole investigations. These investigations revealed the presence of five nearly horizontal layers. Field and laboratory tests were conducted to characterize the ground conditions for the project. The drilled boreholes encountered multiple subsurface layers. The uppermost layer, L1, consists of sandy lean clay (CL) with brown sand and

clay, along with lime gravel and cobbles, ranging in thickness from 1.45 to 1.50 m. Immediately below L1 is layer L2, the composition of the sedimentary formation consists primarily of fat clay (CH), accompanied by brown to reddish brown clay and sporadic occurrences of lime gravel and cobbles with a thickness of 2.9 to 3.0 m. Layer L3, clayey sand (SC), is brown to reddish brown and contains scattered gravel and cobbles of limestone, with a thickness ranging from 6.35 to 6.50 m. Layer L4, elastic silt (MH), the soil in this area exhibits a brown to reddish-brown silt texture and contains a mixture of gravel and cobbles of limestone, ranging from 5.8 to 6.0 m in thickness.

Finally, layer L5 is gravelly fat clay with sand (CH), consisting of grayish creamy clay with sand and gravel. The geological formation in this area consists of fractured dolomitic limestone, which has moderate to strong strength. It is interspersed with layers of yellowish creamy, fractured marly limestone that ranges from weak to moderately weak, often containing nodules and fossils. Additionally, there are thin layers of marl that exhibit a very weak to weak strength.

### 2.3. Soil nail system construction procedures

The excavation process was meticulously carried out following a well-defined work plan to ensure the safe and efficient progress of the project. It was systematically divided into multiple stages, allowing for careful monitoring and control at every step. After each excavation stage, ground nails were promptly and securely installed to provide crucial support for the diaphragm. Subsequently, steel reinforcing elements (nails) were meticulously incorporated to further enhance the structural stability. The thoughtful placement of a geogrid layer followed, serving as an additional reinforcement measure. The application of sprayed concrete was carried out precisely, providing enhanced fortification for the excavated area. The entire excavation process was methodically divided into five distinct stages, each serving a specific purpose and contributing to the overall progress. For detailed information regarding the precise positioning of the nails within the soil mass, please refer to Figure 2.

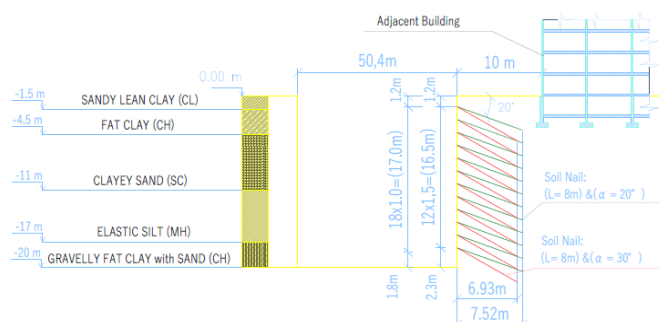


Figure 2. A section of the excavation wall and the geometric parameters of soil nails and Soil layers in sit

Initial data. Excavation with a depth of 20 m has dimensions in terms of 48×50 m with vertical walls without a slope. On Figure 2 shows the geological characteristics of soils at the construction site. The construction of the excavation and foundations, as well as the entire cycle of works on the construction of the underground part of the building, including the stage of backfilling with soil, is scheduled for the summer period. This condition will ensure a reduction in labor and material costs at the stage of fixing the walls of the excavation. Figure 1 shows the plan of the area of the construction site.

The load from the building on the left side of the excavation is calculated as a static surface load of 35 kN/m<sup>2</sup>, on the right sides – the distances to existing buildings are significant, so a wall with a greater load was chosen for analysis. To stabilize the excavation walls, a method involving dowel fastening of the soil massif (drilled nails) with a protective coating on the wall surface (slope) was implemented.

The length of the nails was set at 8 meters, which corresponds to 0.4 times the height of the excavation. The protective coating on the wall surface consists of a layer of geogrid followed by a 50 mm thick application of concrete coating. Various models were created with different dowel spacing and angles of inclination. In all models, the first row of nail was installed at a depth of 1.2 meters.

The construction process for a soil nail wall involves several steps. Initially, an excavation is performed, typically ranging in depth from 91.44 to 152.40 cm, with the front side left unsecured until the installation of nails and initial cladding. Specialized drilling equipment is used to drill holes for the nails, which are then installed and grouted. Strip drains are also placed on the excavation face. Subsequently, an initial layer of shotcrete is applied to the unsupported cut. This layer is composed of a blend of welded-wire mesh and strategically positioned horizontal and vertical bars surrounding the nail heads, aiming to enhance the resistance to bending. The careful arrangement of these components serves the primary objective of reinforcing the structure against bending forces. Upon the complete curing of the shotcrete, a steel bearing plate is meticulously positioned over the exposed tendon, while the nail head is securely fastened against the bearing plate using hex nuts and washers. Select nails may undergo proof-load testing to validate their load-bearing capacity. This sequential procedure is replicated for each subsequent excavation lift, allowing the downward extension of the strip drain and the continuation of the temporary shotcrete from the previous lift. As the excavation reaches its ultimate depth, the nails are systematically installed, and subjected to rigorous testing, and a permanent facing is erected using reinforced shotcrete [24].

Geometric characteristics of numerical models.

Model 1. A control model without the use of reinforcing elements was performed to compare the results obtained.

Model 2. Pin spacing 1.0×1.0 m with pin inclination 20°.

Model 3. Pin spacing 1.0×1.0 m with pin inclination 30°.

Model 4. Pin spacing 1.5×1.5 m with pin inclination angle 20°.

Model 5. Pin spacing 1.5×1.5 m with pin inclination angle 30°.

Model 6. Pin spacing 2.0×2.0 m with pin inclination 20°.

Model 7. Pin spacing 2.0×2.0 m with pin inclination 30°.

Model 8. Pin spacing 3.0×3.0 m with pin inclination 20°.

Model 9. Pin spacing 3.0×3.0 m with pin inclination 30°.

For all models, the calculation was performed using the Hardening Soil Model (HS-model) system and the results were analyzed. For modeling, used common staged construction (CSC). The depth of excavation is shown in Figure 3.

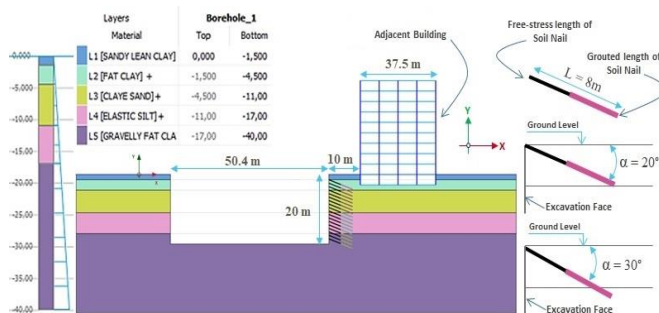


Figure 3. Numerical simulation model of a 20 m soil stud wall and boundary conditions

Figure 3 shows a model of the excavation wall with soil nails, including the geometric characteristics of the excavation and the parameters of the soil nails, the soil layers at the excavation site, the boundaries of the grid, and the fixation conditions.

### 3. Numerical analysis

Numerical analysis is an essential aspect of geotechnical engineering as it enables the simulation of soil behavior under different conditions. In the context of deep excavations supported by a soil nail system, the HS-model incorporates various parameters to accurately represent soil behavior and ensure the design of safe and stable structures [25].

These parameters are crucial for finite element analysis, as they determine the stiffness properties and other important soil characteristics required for the simulation. One of the key parameters in the HS-model is the effective secant modulus ( $E_g$ ), which represents the soil's modulus of elasticity at a 50% stress level under confining conditions. This parameter is determined through a series of drained triaxial compression tests conducted on soil samples indicated in Table 1.

The relationship between the mean stress ( $\sigma_m$ ), the vertical effective stress ( $\sigma_v$ ), and the stress exponent ( $m$ ) – is described by Equation 1 for normally consolidated soils and Equation 2 for over consolidated soils:

$$E_g = E_{50}^{ref} \cdot \left( \frac{\sigma_m}{\sigma_v} \right)^m ; \tag{1}$$

$$E_g = E_{50}^{ref} \cdot \left( \frac{\sigma_m}{\sigma_o} \right)^m . \tag{2}$$

Table 1. Mechanical and physical properties of soil layers

Layer No.	Properties		Shear strength							Vertical coefficient of consolidation, $C_v$ , [ $\cdot 10^{-2}(\text{cm}^2/\text{s})$ ]	Horizontal coefficient of consolidation, $C_h$ , [ $\cdot 10^{-2}(\text{cm}^2/\text{s})$ ]	Standard penetration test, $N$ , No. of blows
	Void ratio, $e$	Porosity, $n$	Direct shear		Consolidated undrained, triaxial		Unconsolidated undrained, triaxial		Unconfined compression strength, $q_u$ , kPa			
			Friction angle, $\phi^\circ$	Cohesion, $c$ , kPa	Friction angle, $\phi^\circ$	Cohesion, $c$ , kPa	Friction angle, $\phi^\circ$	Cohesion, $c$ , kPa				
L1	1.02	0.50	13	25	14	30	0	45	69	2.37	3.21	10
L2	1.25	0.55	10	21	13	36	0	34	61	0.89	1.12	3
L3	1.05	0.51	15	10	22	5	0	64	89	–	–	11
L4	1.44	0.59	–	–	22.3	36	0	39	66	5.12	6.45	5
L5	1.04	0.5	15	17	32	5	0	69	94	–	–	19

In both equations, ( $E_g$ ) represents the modulus of elasticity of the soil, ( $E_{50}^{ref}$ ) is the effective secant modulus at a 50% stress level, ( $\sigma_m$ ) is the mean stress, ( $\sigma_v$ ) is the vertical effective stress, ( $\sigma_o$ ) is the pre-consolidation stress, and  $m$  is the stress exponent. The choice between Equation (1) and Equation (2) depends on the consolidation state of the soil. In the case of dry soil, which typically has low moisture content and is not consolidated significantly, normally consolidated soil behaviour is more appropriate. The stress exponent ( $m$ ) this statement originates from the outcomes of triaxial compression experiments. or oedometer tests and reflects the stress-strain behavior of the soil. It indicates how the soil's stiffness or modulus changes with varying stress levels. Both ( $E_{50}^{ref}$ ) and ( $E_{ode}^{ref}$ ) are parameters obtained from consolidation tests, representing the effective secant modulus of the soil at different stress levels [26]. It is worth noting that if the unloading-reloading cycle is not performed during the triaxial test, some numerical analysis software may apply a multiplier of three to the value of ( $E_{50}^{ref}$ ) to estimate ( $E_{ode}^{ref}$ ). In

numerical analysis software, The coefficient of at-rest earth pressure ( $k_o^{nc}$ ) is approximated as  $(1 - \sin\phi')$ , where ( $\phi'$ ) represents the effective angle of internal friction. This simplification aids in modeling soil behavior, particularly for normally consolidated soils. The angle of dilatation ( $\psi$ ) is another parameter used in numerical analysis. For undrained analysis, ( $\psi$ ) is typically assumed to be zero, indicating no volumetric change during loading. For drained analysis, ( $\psi$ ) is approximated as  $(\phi' - 30^\circ)$ ; considering the influence of soil dilatation on analysis. The unloading-reloading Poisson's ratio ( $V_{ur}$ ) is commonly set equal to 0.2 in numerical analysis, reflecting the change in lateral strain during unloading and reloading [27] By employing these equations and input parameters, the PLAXIS 2D Connect Edition v22 program accurately simulates the stress-strain state of the soil during excavation. The software employs a computational method specifically designed for analyzing two-dimensional plane-strain and using finite element techniques model to provide insights into the soil's behavior. Table 2 presents a summary of the main input parameters for the soil layers used in the numerical simulation of the coordinated model within the HS-model.

Table 2. Soil layers parameters for HS-model

Layer No.	Soil unit weight, $\gamma$ , kN/m <sup>3</sup>	Secant stiffness in drained triaxial, $E_{50}^{ref}$ , kN/m <sup>2</sup>	Tangent oedometric modulus, $E_{ode}^{ref}$ , kN/m <sup>2</sup>	Unloading/reloading stiffness, $E_{ru}^{ref}$ , kN/m <sup>2</sup>	Stress exponent, $m$	Cohe-sion, $c$ , kN/m <sup>2</sup>	Internal friction, $\phi^\circ$	Effective friction angle, $\phi'$	Dilatation angle, $\psi^\circ$	Coefficient of earth pressure at rest, $K_o^{nc}$	Unloading/reloading Poisson's coefficient, $V_{ur}$
L1	18.5	14600	14600	43800	0.8	15.0	14.0	0	0	0.501	0.2
L2	17.7	11550	11550	63525	0.5	18.0	13.0	0	0	0.501	0.2
L3	18.0	23700	23700	71100	0.5	2.50	22.0	0	0	0.515	0.2
L4	17.4	22900	22900	45800	0.6	18.0	22.3	0	0	0.515	0.2
L5	18.4	35400	35400	88500	0.5	5.50	23.5	0	0	0.515	0.2

To determine the soil nail parameters by calculation  $T_{skin, start, max}$  using Equation (3). This equation establishes a relationship between the initial skin friction observed during loading and various factors, including the strength and diameter of the reinforcing steel, the diameter of the drill hole, the modulus of elasticity of the soil, and the angle of internal friction of the soil:

$$T_{skin, start, max} = \left( \frac{F_y \cdot D}{E_g} \right) \cdot \left( 1 - \frac{D}{DDH} \right) \tan \phi, \quad (3)$$

where:

$T_{skin, start, max}$  – the maximum skin friction at the start of loading;

$F_y$  – the yield strength of the reinforcing steel;

$D$  – the diameter of the reinforcing steel;

$E_g$  – the modulus of elasticity of the soil;

$DDH$  – the diameter of the drill hole;

$\phi$  – the angle of internal friction of the soil.

Equation (3) accounts for the fact that skin friction develops primarily at the interface between the reinforcing steel and the soil. When a load is applied, skin friction is mobilized and reaches its maximum value at the beginning of the load. The formula takes into account the influence of the diameter of the reinforcing steel and the diameter of the hole on the skin. The formula also includes the influence of the modulus of elasticity of the soil on the friction of the skin.

The yield strength ( $F_y$ ) of reinforcing steel can be calculated using the following Equation (4):

$$F_y = \frac{F}{A}, \quad (4)$$

where:

$F$  – the applied force or load;

$A$  – the area of the steel cross section.

The yield strength is the maximum stress that steel can withstand without permanent deformation. The formula also takes into account the effect of soil elasticity modulus on surface friction. The equivalent elastic modulus ( $E_{ec}$ ) of grouted nails can be determined taking into account the elastic stiffness of both the grout cover and the rebar. Equation (5) for calculating ( $E_{ec}$ ) is as follows:

$$E_{ec} = \frac{(E_c \cdot A_g) + (E_s \cdot A_c)}{(A_g + A_s)}, \quad (5)$$

where:

$E_c$  – the elastic modulus of the cement slurry;

$A_g$  – cross sectional area of the cement pavement;

$E_s$  – the elastic modulus of the rebar;

$A_c$  – the cross-sectional area of the grout cover;

$A_s$  – cross sectional area of the rebar [24]-[26].

After determining the equivalent elastic modulus ( $E_{eq}$ ) using this equation, the axial hardness ( $E_A$ ) and resistance

bending ( $E_I$ ) of cemented nails can be calculated using Equations (6) and (7):

$$E_A = E_{eq} \cdot I ; \tag{6}$$

$$E_I = E_{eq} \cdot I , \tag{7}$$

where:

- $A$  – the cross sectional area of the nail;
- $I$  – the moment of inertia of the cross-section of the nail;
- $E_{eg}$  – the modulus of elasticity of the cement slurry;
- $E_n$  – the elastic modulus of the nail;
- $E_{eq}$  – the equivalent elastic modulus of the poured soil nail;
- $A_n$  – cross sectional area of the reinforcing bar;
- $A$  – ross sectional area of the poured ground nail;
- $A = (\pi DDH^2) / 4$ ;
- $A_n = (\pi D^2) / 4$ ;
- $A = (A - (A_n))$ .

$$[Axial - hardness] E_A = \left( \frac{E_{eq}}{S_h} \right) \cdot \left( \frac{\pi DDH^2}{4} \right); \tag{8}$$

$$[Resistance - bending] E_I = \left( \frac{E_{eq}}{S_h} \right) \cdot \left( \frac{\pi DDH^2}{46} \right), \tag{9}$$

where:

$DDH^2$  – is the diameter of the drill hole.

Table 3 provides a comprehensive summary of the parameters and material properties associated with the nail system in the numerical simulation of the coordinated model within the HS-model.

**Table 3. Parameters and material properties of the nail system for HS-model**

Parameters	Symbol	Value	Unit
Material type	–	Elastic	–
Axial hardness	$E_A$	$228.707 \cdot 10^3$	kN/m
Resistance to bending	$E_I$	142.9419	kNm <sup>2</sup> /m
Yield point strength	$F_y$	415	MPa
Elastic modulus	$E_n$	200	GPa
Elastic modulus of the cement slurry (concrete)	$E_c$	20	GPa
Diameter of the reinforcing steel	$D$	20	mm
Drill hole diameter	$DDH$	100	mm
Length of nail	$L$	8	m
Declination with respect to horizontal	$\theta$	20° and 30°	degree
Spacing	$S_h \cdot S_v$	[1×1], [1.5×1.5], [2×2] and [3×3]	m
Facing thickness	$t$	200	mm

Based on the information provided, the wall of the excavation is treated as a plane strain problem. The behavior is modeled under dry conditions. The finite element mesh used consists of 15-noded triangular elements, which are generated with an appropriate density. A fine mesh density is highly informative, and it additionally reduces the density near the soil nail wall (Fig. 4).

The grid boundaries are located at a sufficient distance to minimize their influence on the results of numerical simulation, in accordance with the approach described in [28].

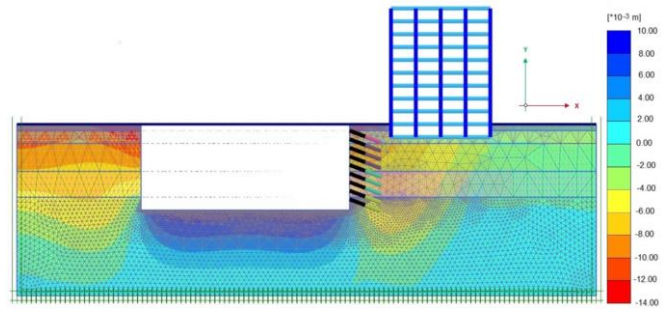


**Figure 4. The mesh for the deep excavations geometry of the soil nail wall to simulate its behavior**

### 3. Numerical results and discussion

In this study, numerical simulations were performed, and the obtained results were compared and validated with the data and findings from the previous study conducted by [29]. The comparison of the results from this study, the measurement data, and the results from reference [29] was performed at the final stage of the excavation, as depicted in Figure 5.

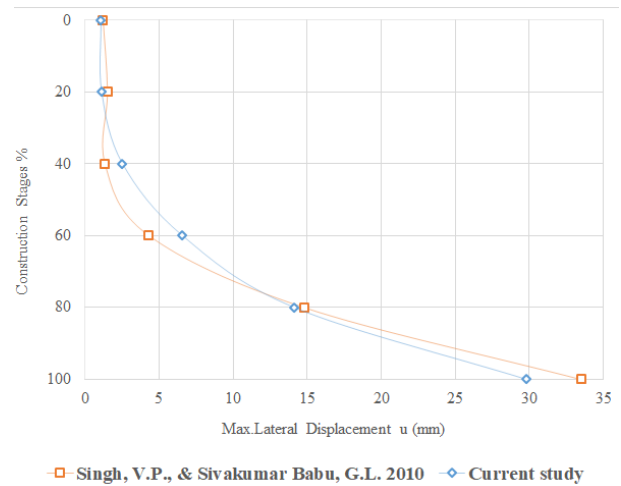


**Figure 5. Comparison of results between the current study and [29]**

The results are evident from Figure 5 demonstrate that the results of the study presented in this article are largely comparable with the results obtained in the study [29]. Specifically, the deflection “u” at the edge of the excavation was found to be 30 mm in the current study and 34 mm in the study [29]. The comparison between the results of the current study and the findings of references [29] indicates a significant agreement between them. It should be noted that the previous study investigated the angle of nails at an inclination of 15 degrees and the excavation depth of 10 meters. Therefore, in our study, we specifically conducted excavations up to a depth of 10 meters for accurate comparison purposes. This approach ensures the precision and reliability of our model. Numerical models with different geometric characteristics are analyzed based on the graphs of horizontal and vertical deformations, as the main indicators in calculating the stability of the excavation wall. The results of changes in the horizontal and vertical displacements of the excavation wall for models of soil nails are presented in Figures 6 and 7 respectively.

It is possible to single out the parameters of reinforcement with nails, which have the greatest impact on the stability of the deep wall of the excavation in rapidly drying soils.

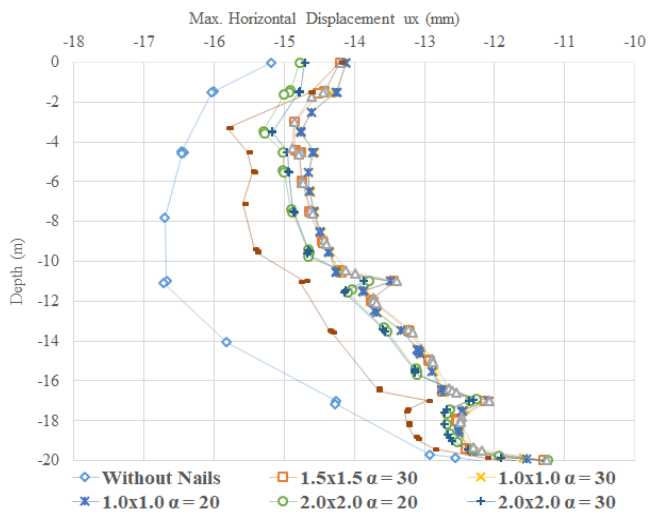


**Figure 6. Horizontal displacement of the wall for various soil nail arrangements**

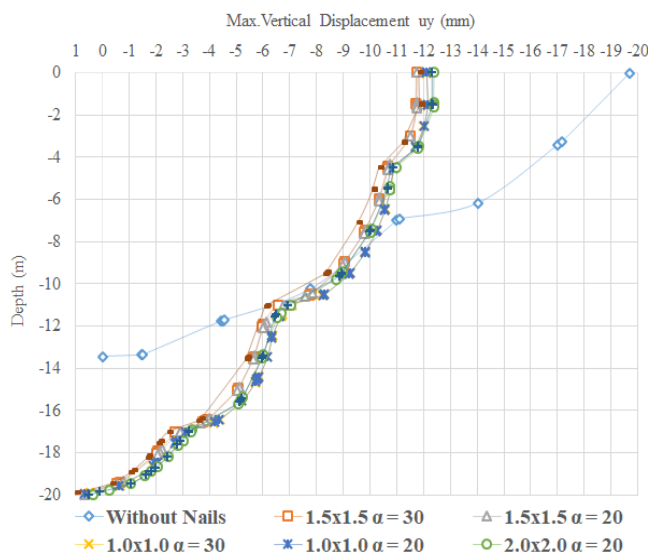


**Figure 7. Vertical displacement of the wall for various soil nail arrangements**

Namely: the length of the nail, the distance between the nails, the angle of inclination of the nail and the coefficient of friction at the soil-nail interface. In this study, the effect of nail spacing, nail angle, and soil-nail friction coefficient on the stability of a deep excavation wall in rapidly drying soils was analyzed. The length of the nail remained constant and was set to the minimum allowable for the given depth of the excavation. To determine which of these parameters has the greatest impact on the stability of the excavation wall, appropriate analyzes and calculations were carried out. The finite element method was used to model the behavior of soil and nails under loads caused by excavation. Based on the results obtained, a comparative analysis of models with different configurations of parameters for reinforcing the wall of the excavation with nails was carried out. It was found that the coefficient of friction at the soil-nail interface has a significant impact on the stability of the excavation wall when using nail reinforcement. The stability of the excavation wall is higher at higher values of the coefficient of friction, which ensured efficient transfer of forces from the nails to the ground. In turn, at a lower value of the friction coefficient, the nails do not effectively transfer the load to the ground,

which leads to an increase in deformations and a possible collapse of the excavation wall. The influence of this parameter on the stability of the structure is clearly seen in Figure 6, as well as on the site soil profile shown in Figure 3. Thus, by analyzing the properties of the soil layers, the top layer L1 (SANDY LEAN CLAY) and the L5 layer (GRAVEL OIL CLAY with SAND) are more stable than the middle layers L2 (GAT CLAY) and L3 (CLAY SAND), which are softer and more subject to deformation. The bottom layer L4 (ELASTIC SLUT) is also relatively stable. The maximum horizontal deformation is determined in the middle layers L2 (GAT CLAY) and L3 (CLAY SAND). The maximum vertical deformation is defined in layer L2 (GAT CLAY). What we observe in Figure 6 and 7. An important role in strengthening the wall of the excavation in quick-drying soils is played by the angle of inclination of the nails. The influence of the angle of installation of the nails on the wall of the excavation is as follows.

Stability – increasing the angle of the nails increased the stability of the excavation wall, especially in the presence of quick-drying soils.

The steeper angle of the nails creates more horizontal force, which helps resist ground pressure and prevents wall movement. Distance between nails.

A steeper angle of inclination allows for greater spacing between nails, which can be beneficial in terms of material savings and installation costs.

Interaction with the earth. The angle of the nails can also affect how the nails interact with the ground. A steeper angle of inclination can create more friction between the dowel and the ground, which can aid soil retention. In all models considered in this study, there is an improvement in the stability of the soil nailed wall with an increase in the angle of inclination of the nails.

The influence of the distance between the nails on the stability of the excavation wall in quick-drying soils can be different. Reducing the distance between the nails led to an improvement in the stability of the excavation wall. This is due to the fact that a denser placement of nails allows better control of soil deformations and prevents its movement. Reducing the distance between the nails increased the resistance of the soil to horizontal deformations, which will reduce the likelihood of collapse of the excavation wall.

Wall displacement is a crucial safety factor that affects both the support system and nearby structures. In underground construction, it is common to observe horizontal wall displacement of up to 2% of the final depth of excavation [30], [31]. However, this range of horizontal displacement is not suitable when shoring is in close proximity to a neighboring building or structure. Through their study [32] found that the maximum lateral wall displacement, based on case histories, was approximately 0.2% of the excavation depth. Usually, the permissible horizontal deformations of the excavation wall are from 0.1 to 0.5% per 1 meter of the excavation width.

Thus, with an excavation width of 48 meters, the allowable horizontal deformations of the excavation wall range from 48 to 240 mm. In general, allowable vertical deformations are usually a few percent of the excavation depth. For a deep excavation 20 meters deep, allowable vertical deformations can be in the range of 0.5 to 2.0% of the excavation depth. This means that allowable vertical deformations in those studies can be between 100 and 400 mm for this case.

Based on the findings [33], the maximum lateral displacement of soil nailed walls typically does not exceed 0.2%. The maximum lateral (horizontal) displacement of the soil-nailed wall models investigated in this study is illustrated in Figure 6. According to the conventional design procedure, for a vertical soil nail wall with sandy soil behind it, the maximum horizontal displacements at the top of the wall are approximately 40 mm for a wall height of 20 m, which corresponds to a displacement ratio of 1/500 of the wall height.

For a general assessment, we compare the results obtained from numerical simulation with the values of permissible horizontal and vertical deformations from general practice and design standards. However, the exact allowable strain values need to be determined in each case based on geotechnical design and engineering calculations. As a result of numerical simulation, it was determined that the maximum horizontal displacement values range from -14.69 mm (model 3) to -15.8 mm (model 9), and the vertical displacement values from -11.734 mm (model 4) to -12.33 mm (model 7).

The above results illustrate the effectiveness of ground nail walls designed according to the traditional design procedure, as well as the ability of ground nail walls to withstand vertical cuts. Comparing models 3, 5, 7 and 9 with each other, it can be seen that the horizontal displacements changed as follows: the decrease between -14.86 (model 5)

and -14.69 (model 3) is -1.16%; the decrease between -15.17 (model 5) and -14.86 (model 7) is -2.08%; the decrease between -15.8 (model 9) and -15.17 (model 7) is -4.14%. Thus, the values decrease by about 1.16, 2.08 and 4.14% between each other, respectively, with increasing distance between the nails. The results of changes in the vertical displacements of the wall for various models are shown in Figure 7. The maximum vertical deformation determines at the upper boundary of layer 2 (at elevations from -1.54 to -1.63) and is in the range from -11.734 (model 4) to -12.33 mm (model 7).

As we see in Figure 7, changing the distance between the nails and their angle did not significantly change the indicators of vertical deformations. This suggests that these factors may not be the dominant factors influencing vertical deformations in the given context. However, it is worth noting that the change in the nature of plotting the graph of vertical and horizontal deformations can be traced with a change in the soil layers of the models. This suggests that the composition and characteristics of the soil layers to the greatest extent determine the deformation behavior of the system.

The clarity of the analysis results, the indicators of maximum horizontal and vertical displacements for models of walls clogged with soil, with different nail spacing and angle of inclination, as well as an indication of the soil layer of the model, are shown in Tables 4 and 5, respectively.

**Table 4. Analysis of maximum horizontal displacement for models soil-nailed walls with different nail spacing and angle of inclination**

Number of models	1	2	3	4	5	6	7	8	9
Space between nails, m	Without nails	1×1	1×1	1.5×1.5	1.5×1.5	2×2	2×2	3×3	3×3
Angle, degree	–	20°	30°	20°	30°	20°	30°	20°	30°
H from top, m	-1.11	-3.51	-3.48	-4.32	-3.01	-3.46	-3.53	-3.42	-3.32
Layer number	L1	L2	L2	L2	L2	L2	L2	L2	L2
Maximum lateral (horizontal) displacement	-16.7	-14.76	-14.69	-14.89	-14.86	-15.3	-15.17	-15.63	-15.8

**Table 5. Analysis of maximum vertical displacement for models soil-nailed walls with different nail spacing and angle of inclination**

Number of models	1	2	3	4	5	6	7	8	9
Space between nails, m	Without nails	1×1	1×1	1.5×1.5	1.5×1.5	2×2	2×2	3×3	3×3
Angle, degree	–	20°	30°	20°	30°	20°	30°	20°	30°
H from top, m	0	-1.63	-1.59	-1.42	-1.41	-1.54	-1.54	-1.57	-1.60
Layer number	L1	L2	L2	L1	L1	L2	L2	L2	L2
Maximum vertical displacement	-19.7	-12.16	-12.11	-11.74	-11.73	-12.33	-12.32	-11.88	-11.85

The study introduces a fresh perspective on soil nail behavior in deep excavation operations, thereby enhancing innovative and rational design methodologies to elevate stability and efficiency. This holds particular significance in regions characterized by rapid soil drainage.

By strategically adjusting nail spacing, angles, and length, this research contributes to formulating practical and realistic design strategies that seamlessly align with future sustainability goals across diverse engineering projects.

This endeavor underscores the optimization of material usage in terms of cost-effectiveness and efficient time utilization. By elevating the level of control over stability and deformation, the study seamlessly integrates rational design principles with sustainable engineering practices, exemplifying their synergy in various intricate excavation projects in the future.

#### 4. Conclusions

Based on the results obtained, the following conclusions can be drawn: stability of the soil layer: the top layer L1 (SANDY LEAN CLAY) and the bottom layer L4 (ELASTIC SULT) show higher stability compared to the average softer and more prone to deformation L2 layers (GAT CLAY) and L3 (CLAY SAND).

Maximum horizontal deformation occurs in the middle layers L2 (GAT CLAY) and L3 (CLAY SAND). These layers are more prone to horizontal displacement.

The maximum vertical deformation is observed in layer L2 (GAT CLAY). The characteristics of this layer had a significant impact on the stability of the structure as a whole, showing higher horizontal and vertical deformations compared to other layers.

Changing the angle of the nails influenced the increase in the stability of the wall of the excavation, especially in quick-drying soil. Models with a steeper angle are more stable.

Pin spacing: the distance between the nails affects the stability of the excavation wall in quick-drying soils. Reducing the spacing enhances stability by better controlling soil deformations and preventing movement.

Soil-nailed wall improvement: The use of soil nails improves the stability of the wall. Increasing the angle of inclination of the nails strengthens the wall, and reducing the distance between the nails enhances soil resistance to horizontal deformations.

Comparison with conventional design. The results of the numerical simulation align with the conventional design procedure and demonstrate the efficiency of soil nail walls in supporting vertical cuts.

Influence of soil layers: changes in the soil layers affect the nature of vertical and horizontal deformations. The composition and characteristics of the soil layers play a significant role in determining the deformation behavior of the system. Thus, it was determined that by rationally choosing the distance between the nails and the angle of their inclination, it is possible to achieve significant results in reducing the deformation of the slope of the excavation and, in general, increasing the stability of the structure. This will allow not overestimate the length of the nails, which is often a problem, to ensure acceptable displacements and deformations when calculating the stability of the walls of deep excavations. This is of practical importance for design and construction in confined spaces and safety to the stability and safety of structures.

## References

- [1] Jafari, M., Girgis, H., Woudenberg, N.V., Liao, Z., Rohling, R.N., Gin, K., Abolmaesumi, P., & Tsang, T. (2019). Automatic biplane left ventricular ejection fraction estimation with mobile point-of-care ultrasound using multi-task learning and adversarial training. *International Journal of Computer Assisted Radiology and Surgery*, (14), 1027-1037. <https://doi.org/10.1007/s11548-019-01954-w>
- [2] Wujun, X. (2012). Applications of ring beam supporting system in deep excavations. *Soil Engineering and Foundation*.
- [3] Kozyukova, N.V., Zhambakina, Z.M., Akishev, U.K., & Sarsenbaev, N.B. (2021). Impact of the stress-strain state of the soil on the stability of the retaining wall. *Journal of Physics: Conference Series*, 1926(1), 012067. <https://doi.org/10.1088/1742-6596/1926/1/012067>
- [4] Bekbergenov, D., Jangulova, G., Kassymkanova, K. K., & Bektur, B. (2020). Mine technical system with repeated geotechnology within new frames of sustainable development of underground mining of caved deposits of the Zhezkazgan field. *Geodesy and Cartography*, 46(4), 182-187. <https://doi.org/10.3846/gac.2020.10571>
- [5] Bondarenko, N., & Tiutkin, O. (2022). Critical analysis of approaches to determining the stress-strain state of the "horizontal working – layered massif" system. *Bridges and Tunnels: Theory, Research, Practice*, (22), 5-11. <https://doi.org/10.15802/bttrp2022/268182>
- [6] Lei, G., Guo, P., Hua, F.X., Gong, X., & Luo, L. (2021). Observed performance and FEM-based parametric analysis of a top-down deep excavation in soil-rock composite stratum. *Geofluids*, (2021), 6964940. <https://doi.org/10.1155/2021/6964940>
- [7] Tabaroei, A., Sarfarazi, V., Pouraminian, M., & Mohammadzadeh, S.D. (2022). Evaluation of behavior of a deep excavation by three-dimensional numerical modeling. *Periodica Polytechnica Civil Engineering*, 66(3), 967-977. <https://doi.org/10.3311/PPci.20353>
- [8] Hou, Y.M., Wang, J., & Zhang, L. (2007). Three-dimensional numerical modeling of a deep excavation adjacent to shanghai metro tunnels. *International Conference on Conceptual Structures*, (4489), 1164-1171. [https://doi.org/10.1007/978-3-540-72588-6\\_184](https://doi.org/10.1007/978-3-540-72588-6_184)
- [9] Tangri, A., & Rawat, S. (2021). Study of stress-strain behaviour in soil nail wall using flexible facing. *IOP Conference Series: Earth and Environmental Science*, (795), 012039. <https://doi.org/10.1088/1755-1315/795/1/012039>
- [10] Lian-xi, L. (2008). Statistical analysis of the surface settlement regulation around deep excavations.
- [11] Li, M., Xiao, X., Wang, J., & Chen, J. (2019). Numerical study on responses of an existing metro line to staged deep excavations. *Tunneling and Underground Space Technology*, (85), 268-281. <https://doi.org/10.1016/j.tust.2018.12.005>
- [12] Haeri, H., Sarfarazi, V., Hedayat, A., & Tabaroei, A. (2016). Effect of tensile strength of rock on tensile fracture toughness using experimental test and PFC2D simulation. *Journal of Mining Science*, (52), 647-661. <https://doi.org/10.1134/S1062739116041046>
- [13] Tian, W., Meng, J., Zhong, X., & Tan, X. (2021). Intelligent early warning system for construction safety of excavations adjacent to existing metro tunnels. *Advances in Civil Engineering*, (2021), 8833473. <https://doi.org/10.1155/2021/8833473>
- [14] Dychkovskiy, R. (2001). Mathematical modeling of geometrical parameters influence of intense fields on intense-deformed condition of massif. *Proceedings of the International Symposium on Geotechnological Issues of Underground Space Use for Environmentally Protected World*, 167-170.
- [15] Chheng, C., & Likitlersuang, S. (2018). Underground excavation behaviour in Bangkok using three-dimensional finite element method. *Computers and Geotechnics*, (95), 68-81. <https://doi.org/10.1016/j.compgeo.2017.09.016>
- [16] Marr, W.A., & Hawkes, M. (2010). Displacement-based design for deep excavations. *Proceedings of the Earth Retention Conference 3*. [https://doi.org/10.1061/41128\(384\)6](https://doi.org/10.1061/41128(384)6)
- [17] Romana Giraldo, J., & Bryson, L.S. (2021). Excavation support system design method to limit damage in adjacent infrastructure. *Journal of Geotechnical and Geoenvironmental Engineering*, 147(12), 1-15. [https://doi.org/10.1061/\(ASCE\)GT.1943-5606.0002677](https://doi.org/10.1061/(ASCE)GT.1943-5606.0002677)
- [18] Wu, L., He, K.Q., Guo, L., & Sun, L. (2022). Analysis of stability law and optimization of slope angle during excavation of deep concave mine slope. *PLoS ONE*, 17(7), e0271700. <https://doi.org/10.1371/journal.pone.0271700>
- [19] Tiutkin, O., Petrosian, N.K., Radkevych, A.V., & Alkhdour, A.M. (2019). Regularities of stress state of unsupported working occurring in a layered massif. *E3S Web of Conferences*, (109), 00100. <https://doi.org/10.1051/e3sconf/201910900100>
- [20] Maleki, M., & Mir Mohammad Hosseini, S.M. (2022). Assessment of the Pseudo-static seismic behavior in the soil nail walls using numerical analysis. *Innovative Infrastructure Solutions*, (7), 262. <https://doi.org/10.1007/s41062-022-00861-5>
- [21] Alkhdour, A.M., Tiutkin, O., Bannikov, D., & Heletiuk, I. (2023). Substantiating the parameters for a non-circular structure of the mine shaft under construction in a heterogeneous rock massif. *IOP Conference Series: Earth and Environmental Science*, (1156), 012008. <https://doi.org/10.1088/1755-1315/1156/1/012008>
- [22] Ou, X., Zhang, X., Fu, J., Zhang, C., Xianshun, Z., & Feng, H. (2020). Cause investigation of large deformation of a deep excavation support system subjected to unsymmetrical surface loading. *Engineering Failure Analysis*, (107), 104202. <https://doi.org/10.1016/j.engfailanal.2019.104202>
- [23] Yong-lai, Z. (2009). Application research on numerical simulation of soil nailing wall for dry dock wall. *Rock and Soil Mechanics*.
- [24] Lazarte, C.A., Robinson, H.D., Gómez, J., Baxter, A., Cadden, A.W., & Berg, R.R. (2015). *Geotechnical engineering circular No. 7 Soil Nail Walls, Reference Manual*. Federal Highway Administration.
- [25] Schanz, T., Vermeer, P.A., & Bonnier, P. (1999) The hardening soil model: Formulation and verification. *Beyond 2000 in Computational Geotechnics*, 281-296. <https://doi.org/10.1201/9781315138206-27>
- [26] Choo Chai, Y. (2016). *Deformation analysis of deep excavation in clay*. PhD Thesis. Queensland, Australia: Griffith University.
- [27] Surarak, T., Likitlersuang, S., Wanatowski, D., Balasubramaniam, A., Oh, E., & Guan, H. (2012). Stiffness and strength parameters for hardening soil model of soft and stiff Bangkok clays. *Soils and Foundations*, 52(4), 682-697. <https://doi.org/10.1016/j.sandf.2012.07.009>
- [28] Briaud, J.L., & Lim, Y. (1997). Soil nailed wall under piled bridge abutment: Simulation and guidelines. *Journal of Geotechnical and Geoenvironmental Engineering*, 123(11), 1043-1050. [https://doi.org/10.1061/\(ASCE\)1090-0241\(1997\)123:11\(1043\)](https://doi.org/10.1061/(ASCE)1090-0241(1997)123:11(1043))
- [29] Singh, V.P., & Sivakumar Babu, G.L. (2010). 2D numerical simulations of soil nail walls. *Geotechnical and Geological Engineering*, (28), 299-309. <https://doi.org/10.1007/s10706-009-9292-x>
- [30] Malik, A. A. (2019). Diaphragm wall supported by ground anchors and inclined struts: A case study. *International Journal of Geomate*, 16(57), 150-156. <https://doi.org/10.21660/2019.57.8170>
- [31] Bhatkar, T., Barman, D., Mandal, A., & Usmani, A. (2016). Prediction of behaviour of a deep excavation in soft soil. *International Journal of Geotechnical Engineering*, 11(1), 10-19. <https://doi.org/10.1080/19386362.2016.1177309>
- [32] Liu, G., Huang, P., Shi, J., & Ng, C.W. (2016). Performance of a deep excavation and its effect on adjacent tunnels in shanghai soft clay. *Journal of Performance of Constructed Facilities*, (30), 04016041. [https://doi.org/10.1061/\(ASCE\)CF.1943-5509.0000891](https://doi.org/10.1061/(ASCE)CF.1943-5509.0000891)
- [33] Juran, I. (1985). Reinforced soil systems – Application in retaining structures. *Geotechnical Engineering*, (16), 39-81.

## **Раціональні конструктивні рішення для глибоких котлованів з використанням підпірної стіни та ґрунтовими нагелями**

А. Алхдур, А.А. Ясін, О. Тютюкін

**Мета.** Дослідження спрямоване на оптимізацію конструкції та зменшення довжини ґрунтових нагелів кріплення глибоких котлованів, що розроблюються у ґрунтах з високою водопроникністю. В ньому також досліджуються параметри, що впливають на стійкість схилів складених ґрунтами з високою водопроникністю.

**Методика.** В поєднанні польових і лабораторних даних, які характеризують властивості ґрунтових нагелів, а також моделювання за допомогою розрахункового комплексу, досліджено, яким чином фіксована довжина нагелів, їхній нахил і відстань між ними впливають на стійкість котловану глибиною 20 м, розробленого у ґрунті, що має високу водопроникність.

**Результати.** Результати дослідження доводять, що оптимальні параметри нагелів (відстань між ними та кут їхнього нахилу), визначені для зміцнення стінок глибокого котловану та забезпечують стійкість із мінімальною довжиною. Важливим результатом є те, що стійкість стінок котловану може бути досягнута без необхідності збільшення довжини ґрунтових нагелів. Рекомендовані параметри характеризують систему ґрунтових нагелів довжиною 8 м, кутом нахилу 30° та розміщенням по сітці 1.5×1.5 м.

**Наукова новизна.** Це дослідження представляє новий погляд на структурні характеристики ґрунтових нагелів, визначаючи відстань між ними, кут нахилу та фіксовану довжину. Дослідження пропонує всебічне обґрунтування для визначення параметрів ґрунтових нагелів у ґрунтах з високою водопроникністю під час розробки глибоких котлованів, сприяючи розвитку методів відкритих розробок.

**Практична значимість.** Дослідження пропонує практичні рішення для проєктувальників, які займаються відкритими розробками на схилах, дозволяючи розробляти ефективні та раціональні проєктні рішення, що забезпечують стійкість котловану та запобігають зсуву під час розробки кар'єру, одночасно зменшуючи витрати та тривалість проєкту.

**Ключові слова:** глибокий котлован, параметри нагелів для підпірних стін, PLAXIS 2D Connect Edition v22, скінченно-елементний аналіз, HS-модель